(14) The three geometries for the water dimer were not fully optimized with the CI calculations,[6c] so only the optimized results from the CI potential function can be reported here.
(15) T. R. Dyke and J. S. Muenter, *J. Chem. Phys.*, **60**, 2929 (1974).
(16) For a review, see P. A. Kollman in "Applications of Electronic Structure Theory", H. F. Schaefer III, Ed., Plenum Press, New York, 1977, p 109.
(17) R. D. Nelson, D. R. Lide, and A. A. Maryott, *Natl. Stand. Ref. Data Ser., Natl. Bur. Stand.*, **No. 10** (1967).
(18) (a) J. C. Owicki and H. A. Scheraga, *J. Am. Chem. Soc.*, **99**, 7403 (1977); (b) S. Swaminathan and D. L. Beveridge, *ibid.*, **99**, 8392 (1977).
(19) D. Eisenberg and W. Kauzmann, "The Structure and Properties of Water", Oxford University Press, London, 1969, p 106.

Minimal Basis Set Description of the Structure and Properties of Liquid Water[1]

William L. Jorgensen

Contribution from the Department of Chemistry, Purdue University, West Lafayette, Indiana 47907. *Received September 21, 1978*

Abstract: A Monte Carlo simulation of liquid water at 25 °C has been carried out using an intermolecular potential function derived from ab initio molecular orbital calculations with a minimal basis set (STO-3G). Comparisons are made with results for structural and thermodynamic properties from simulations based on potential functions representative of Hartree–Fock level (HF) and configuration interaction (CI) calculations. The quality of the results for the liquid is not enhanced smoothly as the ab initio calculations become more sophisticated. The STO-3G and CI potentials yield similar descriptions of liquid water, while the HF potential predicts too little structure beyond the first solvation shell and too high an energy. The first peak in the oxygen–oxygen radial distribution function is somewhat too high and displaced to shorter distances with the STO-3G potential than from the experimental or CI results. Nevertheless, the coordination number and energy distribution functions are similar in the simulations with the STO-3G and CI potentials. It is established that reasonable intermolecular potential functions for hydrogen-bonded dimers can be obtained from minimal basis set calculations.

I. Background and Rationale

It has been 10 years since the first computer simulation of liquid water.[3] In view of the great theoretical and experimental interest in molecular liquids, it is surprising that there has not been a mounting surge of simulations for progressively more complex fluids. In fact, the only systems that have been treated other than water and homonuclear diatomics[4] are carbon monoxide,[4,5] ammonia,[6] benzene,[7] *n*-butane,[8] and recently hydrogen fluoride.[9] Of these, the work on the hydrocarbons must be considered preliminary. The slow progress can largely be attributed to the difficulty in obtaining good intermolecular potential functions for the constituent dimers. The functions are obtained in two ways, which may be called empirical and quantum mechanical. The empirical approach involves the use of sums of standard functions, such as Coulomb and Lennard-Jones, parametrized to reproduce *experimental* properties of the monomers and dimers, e.g., dipole moment, vibrational frequencies, geometry, and dimerization energy. Rahman and Stillinger have formulated and used such functions with great success in their molecular dynamics simulations of water.[10] In the quantum mechanical approach, ab initio molecular orbital calculations are performed for many configurations of the dimer. The resultant dimerization energies are then fit to algebraic forms similar to those in the empirical potentials.

The problem with obtaining intermolecular potential functions empirically for systems more complex than water is the availability and reliability of the necessary experimental data. Water is unique in the extent to which it has been studied experimentally. Furthermore, reliable data on the geometries and dimerization energies for dimers in the gas phase are particularly critical and notoriously difficult to obtain. For example, gas-phase experiments did not confirm a linear structure for the water dimer until 1974, and the error bars for the dimerization energy are still ±30%.[12]

A clear advantage to the quantum mechanical approach is that, in principle, any system can be treated. The complications arise from the dependence of the results on the choice of basis set and correlation energy correlations. There are basically four levels of sophistication: (1) minimal basis set, (2) double ζ basis, (3) double ζ plus polarization (DZ + P) or Hartree–Fock limit (HF), and (4) DZ + P plus correlation corrections via configuration interaction (CI) or perturbation theory methods. Clementi and co-workers obtained potentials for the water dimer at levels 3 and 4.[13] The author's original calculations for the hydrogen fluoride dimer were at level 2.[14] It would seem that the quality of the potential functions should increase with the level of ab initio theory. This point has received almost no attention except in Clementi's work[15] and in the study of Swaminathan and Beveridge which used Clementi's potentials.[16] The issue is clouded by what is used to measure "quality". For the present purposes, the criteria can be radial distribution functions and thermodynamic properties, particularly the energy, which may be calculated for the liquid in Monte Carlo (MC) or molecular dynamics simulations. There is distinct improvement in both areas when the CI potential (level 4) is used for water rather than the Hartree–Fock (HF, level 3).[15,16] Thus, the energies of liquid water at 25 °C from MC calculations using the HF and CI potentials are −4.9 and −6.6 kcal/mol, while the experimental value is −8.1 kcal/mol. In addition, the OO radial distribution function from the HF potential reveals essentially no structure beyond the first solvation sphere, whereas the CI results agree with experiment in finding well-defined second and third solvation shells. If these results are interpreted to imply that acceptable intermolecular potential functions can only be obtained at the CI level, then the quantum mechanical approach could only be applied to small systems with limited survey of their potential surfaces in view of the expense of such calculations.

However, it is likely that the discrepancies between the HF and CI results are mainly due to the lower dimerization energy predicted by the CI potential (−5.84 kcal/mol) than the HF (−4.55 kcal/mol). Consequently, it is doubtful that a smooth

0002-7863/79/1501-2016$01.00/0

enhancement of the structural and thermodynamic data would be obtained by altering the potentials from level 1 to level 4 because the respective dimerization energies are roughly −6, −8, −4.5, and −6 kcal/mol.[17] At level 2, e.g., 4-31G and 6-31G basis sets, hydrogen bond energies are substantially too negative. This required scaling the potential function for the hydrogen fluoride dimer in order to match the experimental energy of vaporization for the liquid in MC calculations.[9a] The obvious question is: what would the results be like for water using a potential derived from minimal basis set calculations (level 1)? Additional impetus for such an undertaking is provided by the observation that dimerization energies for hydrogen-bonded systems are generally well predicted by minimal basis set results. For example, Kollman has estimated the dimerization energies of HF, NH_3, and CH_3OH as −5.4, −3.3, and −4.7 kcal/mol based on the best ab initio calculations.[12] The corresponding values from computations with the minimal STO-3G basis set are −5.5, −3.8, and −5.6 kcal/mol, respectively.[17,18] Further encouragement is available from the excellent agreement between experimental and STO-3G values for bond angles in hydrogen-bonded dimers.[12,17] However, a point of concern is that hydrogen bond lengths are underestimated by STO-3G calculations by 0.2–0.3 Å (ca. 10%). In addition, the fine details of the potential surfaces may be inadequately represented owing to the basis set truncation and lack of correlation energy correlations. This point is difficult to test unambiguously. Similar criticisms can be made for empirical potentials. It is also unclear how sensitive the subsequent results for the liquids are to the subtleties.

Overall, it seemed imperative to attempt a simulation of a liquid starting from minimal basis set calculations. Many issues that have been raised in the above discussion could then be addressed. The obvious liquid to pick is water since it has been the most thoroughly studied. At least a more complete picture of the dependence of the results for liquid water on the sophistication of the ab initio calculations could be obtained. If the results were reasonable, then the possibility of generating preliminary intermolecular potential functions for larger systems economically could be investigated. Simple modification of these functions by adding dispersion corrections may prove adequate for studying at least the structural characteristics of complex liquids. The alternative, CI level calculations, is not viable at this time.

II. Computational Details

A. Potential Function. In the preceding paper, a potential function was derived for the water dimer from 291 STO-3G calculations.[2] The results were fit to a 12-6-3-1 potential function using a four point charge model incorporating two pseudo-lone pairs for each water monomer. The standard deviations for the fit of the 12-6-3-1 function to the STO-3G dimerization energies were ca. 0.3 kcal/mol. The function was thoroughly analyzed and found to provide a well-behaved, accurate representation of the STO-3G potential surface for $(H_2O)_2$. In all aspects of these works, the water monomers have been held fixed at their experimental OH separations (0.9572 Å) and HOH angles (104.52°).[19] The four point charge 12-6-3-1 potential was subsequently employed in simulations of liquid water as described here.

B. Monte Carlo Calculations. A Monte Carlo statistical mechanics calculation was executed for a sample of 125 water molecules at 25 °C and at a density of 1 g/cm^3. These are the same conditions as in the MC work of Clementi and Beveridge with the CI and HF potentials.[15b,16] The calculations have all been carried out in the standard manner using the Metropolis sampling algorithm.[20] The details of such computations have been discussed elsewhere. Sophisticated descriptions may be found in the reviews by Wood, Barker and Henderson, and Watts and McGee.[21] A simplified exposition is available in the paper by Jorgensen.[9a] Periodic boundary conditions were employed for the cubic sample. A spherical cutoff at half the length of an edge of the cube was used in evaluating the dimerization energies. As in the earlier studies,[15b,16] no corrections were made to the energy for dispersion and dipole–dipole interactions with molecules beyond the cutoff. For water, these effects have been estimated by Owicki and Scheraga to total −0.15 kcal/mol for a sample size of 64 molecules.[22] Considering the nature of the potential functions, the neglect of three-body and higher order effects, and the statistical fluctuations in MC calculations, the corrections do not have great importance. One molecule was picked and displaced randomly on each move. Translations in all three Cartesian directions and a rotation about one randomly chosen axis were made each time. An acceptance rate of roughly 50% for new configurations was obtained by using ranges of ±0.12 Å for the translations and ±12° for the rotation.

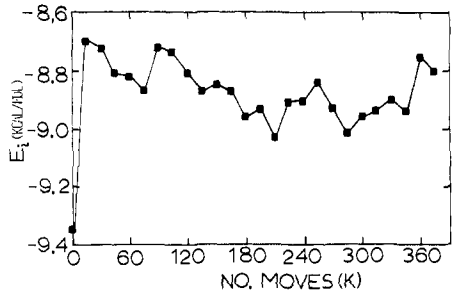

Figure 1. Average energy during each increment of 15 000 attempted moves for the Monte Carlo run with the STO-3G potential. Only the final 300 000 moves were used in the averaging for properties and distribution functions.

The calculation was started from a configuration kindly provided by Professor Beveridge from his study with the CI potential.[16] The convergence of Monte Carlo calculations with Metropolis sampling has received some attention recently.[23,24] The use of the CI configuration was clearly intended to accelerate convergence in contrast to starting with random orientations or an ice configuration. The potential energy of the starting configuration was −9.35 kcal/mol. The MC run was executed in increments of 15 000 (15K) attempted moves. The average energy during each increment is illustrated in Figure 1. The energy immediately rose within the first two increments (30K attempted, 15K successful moves) to ca. −8.7 kcal/mol. During the rest of the run the energy did not vary more than 0.3 kcal/mol from this value. This is consistent with our experience with liquid hydrogen fluoride[9a] in which rapid convergence was found when the MC runs were begun from configurations below the final average energy. Convergence is much slower when the starting configuration has high energy. The first complete oscillation in the energy occurred within 90K attempted moves. Previous experience suggested that this was a signal that equilibration had been achieved. The initial configurations were discarded and the averaging for the structural and thermodynamic properties was performed over the final 300K configurations. The final average energy obtained here (−8.9 kcal/mol) is also consistent with the simulation being near equilibrium. This follows because the CI potential yields a higher energy (−8.6 kcal/mol) which is reasonable in view of the relative dimerization energies from the CI (−5.84 kcal/mol) and STO-3G (−6.46 kcal/mol) potentials.[2]

III. Results and Discussion

A. Radial Distribution Functions. Radial distribution functions, $g_{xy}(r)$, are related to the probability of occurrence

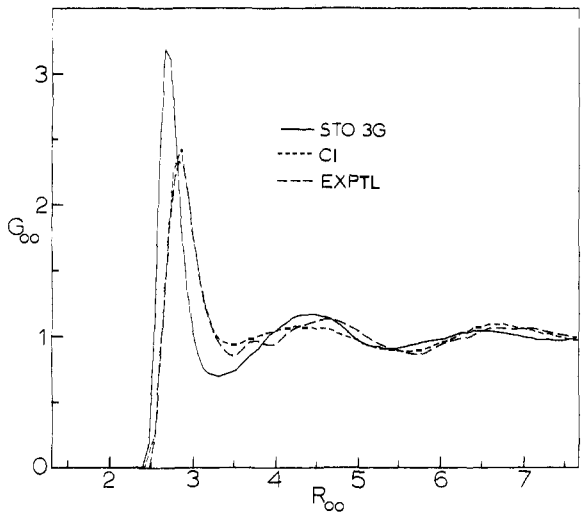

Figure 2. Comparison of OO radial distribution functions for water at 25 °C from simulations with the STO-3G and CI potentials. and from diffraction data.

of atoms with type y at any distance, r, from an atom with type x in the liquid. In MC calculations, $g_{xy}(r)$ is constructed by dividing the range of r into bins, accumulating the occurrences of the interatomic separations for x and y as a histogram, and finally normalizing to adjust for the increasing volume element as r gets large. The proper expression is

$$g_{xy}(R) = \frac{\langle N_y(R, R + \mathrm{d}R)\rangle}{\rho_y 4\pi R^2\,\mathrm{d}R}$$

where the numerator is the average number of y atoms in the shell (bin) between R and $R + \mathrm{d}R$, and ρ is the density. If the density of y atoms at some distance, r', is the same as the overall density of y atoms for the liquid, then $g_{xy}(r') = 1$. Thus, g_{xy} describes the density fluctuations for atoms y about x due to local structure in the liquid. It follows that peaks in g_{xy} are often interpreted as defining solvation shells. Experimentally, radial distribution functions are determined from X-ray and neutron diffraction. Narten et al. have successfully obtained g_{OO} for water at various temperatures in this manner; however, there are ambiguities in acquiring definitive data for g_{OH} and g_{HH}.[25]

The results for g_{OO} from the simulations with the STO-3G and CI potentials[15b] are compared with Narten's data in Figure 2. The CI potential gives the best agreement with experiment for any potential known to date. All three curves in Figure 2 reveal three well-defined solvation shells. The peak positions from the STO-3G results are uniformly biased to shorter distances by 0.17–0.20 Å. The height of the first peak is somewhat exaggerated (3.19 vs. 2.4), though the magnitudes of the subsequent oscillations are fine. These discrepancies are easily traced to the 12-6-3-1 potential, which has its minimum 0.8 kcal/mol below and at 0.22 Å shorter OO separation than the CI potential.[2] Overall, the STO-3G results for g_{OO} compare favorably with the predictions from the empirical potentials used by Rahman and Stillinger and others.[10,21] These functions typically yield heights of 3–4 for the first peak in g_{OO}.[10] In fact, the STO-3G results are very similar to those from the ST2 potential except for the positioning of the first peak.[10b] Most significantly, the g_{OO} from the STO-3G potential is in far better accord with experiment than the results from the Hartree–Fock level potential.[15a] As shown in Figure 2 of ref 16, the HF potential finds the first peak at too large OO separation and predicts g_{OO} to be essentially flat beyond the first peak; in fact, it reveals a slight minimum at the experimental maximum for the second shell.

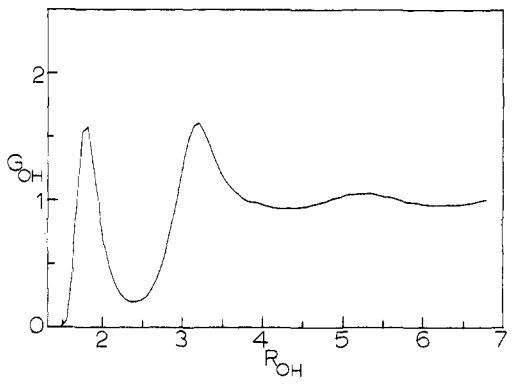

Figure 3. OH radial distribution function for water at 25 °C computed with the STO-3G potential.

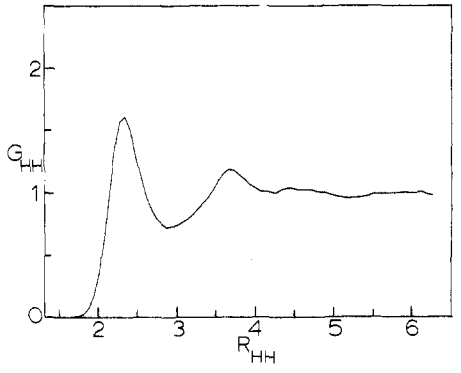

Figure 4. HH radial distribution function for water at 25 °C computed with the STO-3G potential.

The OH and HH radial distribution functions computed with the STO-3G potential are shown in Figures 3 and 4. The results are again similar to those from the ST2 potential. The chief differences with the CI predictions are the sharper definition and height of the first peak in g_{OH} for the STO-3G data. This can be rationalized with reference to Figures 3 and 4 in the preceding paper. It was found that the CI potential has a broader well for the linear water dimer with respect to both the OO separation and the angular variable, θ, than the STO-3G function.[2] So the CI potential is less selective in its preferences for hydrogen-bonding geometries which would in turn yield lower and broader first peaks in g_{OO} and g_{OH}. It seems reasonable that these features are a consequence of the CI potentials's incorporation of dispersion effects. Nevertheless, the small data base (66 points on the water dimer potential surface) used to construct the CI potential makes such rationalizations tentative. As noted before,[2] there is reason to believe that the CI potential is too soft at short range, which would affect the peak shapes in the radial distribution functions.

B. Coordination Numbers. The locations of the minima in the radial distribution functions are associated with the extremities of the corresponding solvation sheaths. Integrating the functions up to these points can then yield estimates of the number of molecules in each shell and therefore average coordination numbers, C. For the first shell with limit R_c

$$C = \int_0^{R_c} g(R)\rho 4\pi R^2\,\mathrm{d}R$$

During an MC calculation, the coordinates of the molecules in the periodic cube are usually saved at regular intervals. When the run is completed and R_c established, the saved configurations can then be analyzed to obtain a detailed

Table I. Distribution of Coordination Numbers

N	C_N, % STO-3G	HF[a]	CI[a]
2	1	7	4
3	11	23	19
4	45	37	47
5	30	23	24
6	10	7	6
7	2	2	0
av	4.55	4.05	4.15
exptl	4.4–4.5[b]		

[a] Data from ref 16. [b] Data from ref 25a.

Table II. Computed Energy and Heat Capacity for Water at 25 °C[a]

	E_i	E	C_v
STO-3G	−8.9	−6.9	12.7
Hartree–Fock[b]	−6.9	−4.9	15.6
CI[b]	−8.6	−6.6	13.5
exptl[c]	−9.9	−8.1	17.9

[a] Energies in kcal/mol; C_v in cal/mol·K. E_i is the configurational potential energy. E and C_v include kinetic energy contributions corrected for quantum effects (see ref 22). [b] Data from ref 15 and 16. [c] Data from ref 11 and 30.

breakdown of coordination numbers by mole fractions. Thus, C_N is defined as the percentage of molecules with coordination number N. The results are displayed by the histogram in Figure 5 for the STO-3G and CI potentials. In this case the analysis has been made from OO separations in the first solvation shell which extends to 3.34 and 3.53 Å for the STO-3G and CI potentials, respectively. The comparison is quantified in Table I, which also includes the data for the HF potential. The predictions from the CI and STO-3G potentials are very similar, though the STO-3G data reveal an enhanced preference for five- and six-coordinated species at the expense of three. In both cases the percentage of four-coordinated water molecules is just under 50%. The distribution for the HF potential is distinctly different. It is nearly symmetric about $N = 4$ with a smaller preference (37%) for four coordination.

The average coordination numbers, C, for the potentials are also compared with the experimental value (4.4–4.5) in Table I. The higher prediction from the STO-3G potential (4.55), expected from the histogram, is in better agreement with experiment than the CI (4.15) and HF (4.05) results. The coordination number is clearly increasing as the well for the linear water dimer deepens in the potential functions. An exact proportionality cannot be expected since the shapes of the wells are certainly influential.

The number of molecules within the limit of the second solvation sheath (5.46 Å) for the STO-3G results is 23.3. An ice I lattice with four coordination predicts 17, while five coordination would yield about 26. This is consistent with the computed coordination number of 4.55. The first peak in g_{OH} (Figure 3) contains 1.9 hydrogens which are presumably functioning as hydrogen bond donors. Since this number is less than 4.55/2, it appears that all nearest neighbors are not strongly hydrogen bonded (vide infra).

C. Thermodynamic Properties. The configurational potential energy (E_i) computed in MC simulations must be augmented by the kinetic energy contributions for comparison with the experimental energy of the liquid. If the translational and rotational energies are treated classically, this would require an addition of $3RT$ (1.8 kcal/mol at 25 °C) to E_i. Analysis of infrared data for water permits the quantum mechanical correction to be estimated as 2.0 kcal/mol at 25 °C.[22] The results for the STO-3G, HF, and CI potentials are compared with experiment[11] in Table II. The computed values are all too positive by 15–40%. Part of the discrepancy is certainly due to the neglect of three-body interactions in the calculations. The effect has been calculated to be constructive and amounts to about 1 kcal/mol per hydrogen bond for sequentially hydrogen bonded water trimers.[27] Including the trimer corrections may then be anticipated to lower the energy of the liquid by ca. 1 kcal/mol. This would bring the STO-3G and CI results in line with experiment. Again, the theoretical values parallel the trend in minimum dimerization energies from the potential functions. It should be noted that standard deviations for the computed energies may be calculated from the fluctuations during MC runs (Figure 1). In each case, the error bars ($\pm 2\sigma$) are ca. ±0.05 kcal/mol.

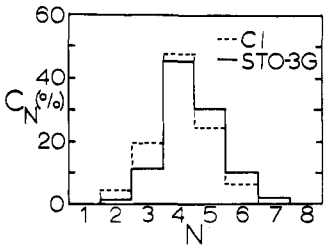

Figure 5. Distribution of coordination numbers within the first solvent shell for water at 25 °C.

Heat capacities are determined in MC studies from the variance of the energy.

$$C_v' = \frac{1}{kT^2}(\langle E^2\rangle - \langle E\rangle^2)$$

This simply requires that both the energy and its square be averaged. The configurational contribution, C_v', must also be adjusted for the kinetic energy contributions. Classically, this amounts to adding $3R$ (6.0 cal/mol·K), while Owicki and Scheraga estimate the quantum correction as 3.6 cal/mol·K for water at 25 °C.[22] The quantum-adjusted values are reported in Table II. The experimental C_v is underestimated by 13–30%. This is again reasonable in view of the assumption of pairwise additivity. Three-body effects would be expected to increase the magnitudes of both the computed E's and C_v's. However, several other issues must be considered before much significance can be attached to the computed C_v's. First, since C_v' is obtained as a variance, the error bars are substantial, ±2 cal/mol·K. Second, it is not clear that the heat capacity converges in as short runs (ca. 500K) as used in the MC simulations that produced the values in Table II.[24] Finally, Berne has shown that an alternative sampling procedure (the force bias method) yields much larger heat capacities than the Metropolis technique.[23] The source and significance of this discrepancy need further examination. For our purposes, it is sufficient to note that the CI and STO-3G potentials provide similar results for the energy and heat capacity of liquid water when used in operationally identical Monte Carlo simulations.

D. Energy Distribution Functions. The format of the MC calculations permits some interesting decompositions for the potential energy of the liquid. The total binding energy for each molecule can be monitored and averaged into a distribution. In view of the pairwise additivity, the total energy is half the sum of the individual binding energies. The binding energy distribution from the MC run with the STO-3G potential is shown in Figure 6. Aside from statistically insignificant ripples, the function reveals a smooth distribution of binding energies from −5 to −28 kcal/mol centered at −18 kcal/mol. That is, on the average, it takes 18 kcal/mol to remove a molecule from

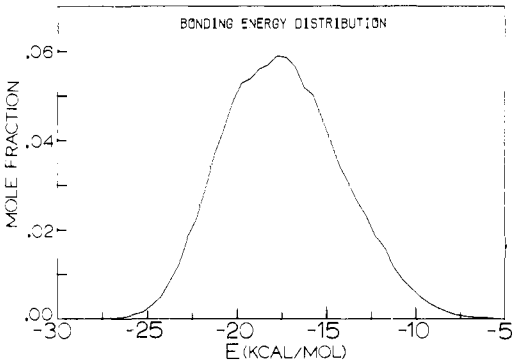

Figure 6. Bonding energy distribution for the monomers in water at 25 °C calculated via the STO-3G potential. The data were collected in bins 0.5 kcal/mol wide. The mole fraction of the molecules in each bin is shown on the y axis.

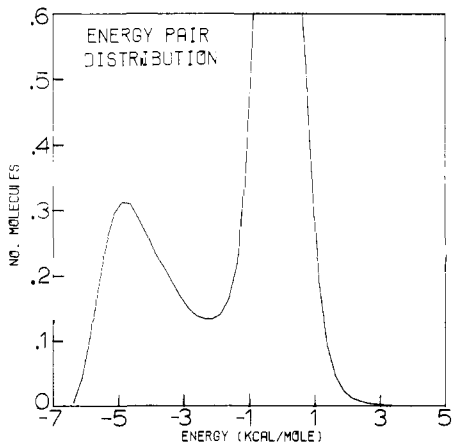

Figure 7. Distribution of dimerization energies in water at 25 °C computed from the STO-3G potential. The data were collected in bins 0.25 kcal/mol wide. The average number of molecules found in each bin is shown on the y axis.

the liquid. This is consistent with the computed potential energy for the liquid of ca. −9 kcal/mol (Table II). The unimodal nature, shape, range, and centering of the STO-3G binding energy distribution are nearly identical with the results of Swaminathan and Beveridge with the CI potential (see ref 16, Figure 8). The HF potential yields a similar curve; however, it is centered at higher energy (−12 kcal/mol), as expected.[16]

Swaminathan and Beveridge discussed the significance of the CI results, so their conclusions apply to the STO-3G data as well. A key point is that the unimodal shape of the distribution argues against interstitial and mixture models for liquid water.[28] In these theories specific molecular clusters would be associated with distinct binding energies which would appear as peaks in the distribution. Consequently, the STO-3G and CI results are consistent with a continuum model for liquid water in which a smooth spectrum of energetic environments is available to the monomers. Similar profiles for binding energies were found in MC simulations of liquid hydrogen fluoride.[9a,c]

The energy from the MC calculation can also be broken down into the distribution of dimerization energies, i.e., how each monomer interacts with the remaining monomers on the average. The STO-3G results are displayed in Figure 7. Naturally, there can be no dimerization energies below the minimum for the potential function (−6.46 kcal/mol).[2] Also, the bulk of the interactions are with distant molecules, so of the 124 molecules interacting with the central monomer 119 yield dimerization energies between ±1 kcal/mol. The interesting feature in the distribution is the peak between −6.5 and −2.0 kcal/mol. Integration shows that the peak contains 3.5 molecules, which accounts for most of the first solvation shell. Thus, the peak is the distribution of dimerization energies for the hydrogen-bonded neighbors. A continuous spectrum of hydrogen bond strengths is indicated. Also not all nearest neighbors are strongly hydrogen bonded. This is reminiscent of the "distorted hydrogen bond" model for water proposed by Pople in 1951.[28,29]

The dimerization energy distribution has not been reported for the CI potential; however, molecular dynamics results with the ST2 potential (ref 10b, Figure 11) are similar to the STO-3G data. A minor difference is that the minimum in the distribution is not as deep from the ST2 calculation. An intriguing feature from the molecular dynamics work is the presence of an invariant point in the distribution at −4 kcal/mol over a temperature range from −3 to 118 °C.[10b] This was interpreted as evidence for a hydrogen bond rupture mechanism involving an equilibrium between pairs with dimerization energies on either side of the point. The only simulation carried out with the STO-3G potential so far has been at 25 °C, so this effect has not been reexamined.

IV. Conclusion

The results of Monte Carlo simulations of liquid water using intermolecular potential functions representative of ab initio calculations with a minimal basis set (STO3G), near the Hartree-Fock limit (HF) and including configuration interaction (CI), have been contrasted here. Comparisons were made for the computed radial distribution functions, distributions of coordination numbers, energy, heat capacity, and energy distribution functions. The STO-3G potential was found to yield uniformly superior results than the HF potential when compared with experiment or with results using the CI potential. The only point clearly favoring the CI potential over the STO-3G alternative is the prediction for the height and location of the first peak in the oxygen-oxygen radial distribution function.

These observations establish that (1) increasing sophistication in the ab initio calculations for the potential functions is not necessarily paralleled by enhancement of the results for the liquid; (2) reasonable intermolecular potential functions for hydrogen-bonded dimers can be generated from minimal basis set calculations. Thus, an economical means for creating preliminary intermolecular potential functions for systems larger than the water dimer appears to be available. Of course, any potential function must be thoroughly tested to guarantee that it is physically reasonable. Furthermore, the potential functions from minimal basis set calculations may require the addition of empirical terms for dispersion corrections so that interactions with nonpolar groups can be fairly represented. As demonstrated here, a critical attribute for a successful potential function is that it provides a good estimate of the dimerization energy.

Finally, it is noted that the comparisons made here based on Monte Carlo calculations have not included properties such as pressure and viscosity which are normally determined in molecular dynamics simulations. It is known that the pressure of liquid water is substantially overestimated with the CI potential.[15b] The STO-3G potential with its shorter OO separation for the water dimer may provide improvement in this respect; however, in the absence of three-body corrections it is improper to expect a true dimer potential to perform well for such properties. Fortunately, static structural features are not as sensitive to the details of the potential functions so fascinating descriptions of molecular liquids can be successfully obtained from simulations with two-body potentials.

Acknowledgments. The author is grateful for receipt of data from Drs. D. L. Beveridge and A. H. Narten. Acknowledgment is made to the donors of the Petroleum Research Fund, administered by the American Chemical Society, for support of this research. Aid from the Dreyfus Foundation, the Purdue Research Foundation, Purdue University Computing Center, and the Deutscher Akademischer Austauschdienst also facilitated this study.

References and Notes

(1) Quantum and Statistical Mechanical Studies of Liquids. 4. Part 3: ref 2.
(2) W. L. Jorgensen, *J. Am. Chem. Soc.*, preceding paper in this issue.
(3) J. A. Barker and R. O. Watts, *Chem. Phys. Lett.*, **3**, 144 (1969).
(4) For a review, see W. B. Streett and K. E. Gubbins, *Annu. Rev. Phys. Chem.*, **28**, 373 (1977).
(5) G. D. Harp and B. J. Berne, *Phys. Rev. A*, **2**, 975 (1970).
(6) (a) I. R. McDonald and M. L. Klein, *J. Chem. Phys.*, **64**, 4790 (1976); (b) D. L. Beveridge et al., to be published.
(7) (a) R. O. Watts and D. J. Evans, *Mol. Phys.*, **32**, 93 (1976); (b) J. Kushick and B. J. Berne, *J. Chem. Phys.*, **64**, 1362 (1976).
(8) J. P. Ryckaert and A. Bellemans, *Chem. Phys. Lett.*, **30**, 123 (1975).
(9) (a) W. L. Jorgensen, *J. Am. Chem. Soc.*, **100**, 7824 (1978); (b) M. L. Klein, I. R. McDonald, and S. F. O'Shea, *J. Chem. Phys.*, **69**, 63 (1978); (c) W. L. Jorgensen, *ibid.*, in press.
(10) (a) A. Rahman and F. H. Stillinger, *J. Chem. Phys.*, **55**, 3336 (1971); (b) F. H. Stillinger and A. Rahman, *ibid.*, **60**, 1545 (1974); (c) *ibid.*, **68**, 666 (1978).
(11) (a) N. E. Dorsey, "Properties of Ordinary Water Substance", Reinhold, New York, 1940; (b) D. Eisenberg and W. Kauzmann, "The Structure and Properties of Water", Oxford University Press, London, 1969.
(12) For a review, see P. A. Kollmann in "Applications of Electronic Structure Theory", H. F. Schaefer III, Ed., Plenum Press, New York, 1977, p 109.
(13) (a) H. Popkie, H. Kistenmacher, and E. Clementi, *J. Chem. Phys.*, **59**, 1325 (1973); (b) O. Matsuoka, E. Clementi, and M. Yoshimine, *ibid.*, **64**, 1351 (1976).
(14) W. L. Jorgensen and M. E. Cournoyer, *J. Am. Chem. Soc.*, **100**, 4942 (1978).
(15) (a) H. Kistenmacher, H. Popkie, E. Clementi, and R. O. Watts, *J. Chem. Phys.*, **60**, 4455 (1974); (b) G. C. Lie, E. Clementi, and M. Yoshimine, *ibid.*, **64**, 2314 (1976).
(16) S. Swaminathan and D. L. Beveridge, *J. Am. Chem. Soc.*, **99**, 8392 (1977).
(17) J. D. Dill, L. C. Allen, W. C. Topp, and J. A. Pople, *J. Am. Chem. Soc.*, **97**, 7220 (1975).
(18) J. E. Del Bene, *J. Chem. Phys.*, **55**, 4633 (1971).
(19) W. S. Benedict, N. Gailar, and E. K. Plyler, *J. Chem. Phys.*, **24**, 1139 (1956).
(20) N. Metropolis, A. W. Rosenbluth, M. N. Rosenbluth, A. H. Teller, and E. Teller, *J. Chem. Phys.*, **21**, 1087 (1953).
(21) (a) W. W. Wood in "Physics of Simple Liquids", H. N. V. Temperley, J. S. Rowlinson, and G. S. Rushbrooke, Eds., Wiley-Interscience, New York, 1968; (b) J. A. Barker and D. Henderson, *Rev. Mod. Phys.*, **48**, 587 (1976); (c) R. O. Watts and I. J. McGee, "Liquid State Chemical Physics", Wiley, New York, 1976.
(22) J. C. Owicki and H. A. Scheraga, *J. Am. Chem. Soc.*, **99**, 8392 (1977).
(23) C. Pangali, M. Rao, and B. J. Berne, *Chem. Phys. Lett.*, **55**, 413 (1978).
(24) D. L. Beveridge et al., to be published.
(25) (a) A. H. Narten, M. D. Danford, and H. A. Levy, *Discuss. Faraday Soc.*, **43**, 97 (1967); (b) A. H. Narten and H. A. Levy, *J. Chem. Phys.*, **55**, 2263 (1971); (c) A. H. Narten, *ibid.*, **56**, 5681 (1972).
(26) Reference 11b, p 165.
(27) (a) J. E. Del Bene and J. A. Pople, *J. Chem. Phys.*, **52**, 4858 (1970); (b) B. R. Lentz and H. A. Scheraga, *ibid.*, **58**, 5296 (1973); (c) D. Hankins, J. W. Moscowitz, and F. Stillinger, *ibid.*, **53**, 4544 (1970).
(28) For a summary, see ref 11b, Chapter 5.
(29) J. A. Pople, *Proc. R. Soc. London, Ser. A*, **205**, 163 (1951).
(30) J. S. Rowlinson, "Liquids and Liquid Mixtures", 2nd ed., Plenum Press, New York, 1969, p 63.

Energy Transfer from Triplet Aromatic Hydrocarbons to Tb^{3+} and Eu^{3+} in Aqueous Micellar Solutions

M. Almgren,† F. Grieser, and J. K. Thomas*

Contribution from the Radiation Laboratory,‡ University of Notre Dame, Notre Dame, Indiana 46556. *Received September 7, 1978*

Abstract: The sensitization of Tb^{3+} and Eu^{3+} luminescence by energy transfer from aromatic triplet donors like naphthalene, bromonaphthalene, biphenyl, and phenanthrene in micellar sodium lauryl sulfate solution has been studied. Formal second-order rate constants for the energy transfer process in the micellar solutions were determined as 5×10^5 and 1.8×10^5 M^{-1} s^{-1} for transfer from 1-bromonaphthalene to Eu^{3+} and Tb^{3+}, respectively, and 4×10^5 M^{-1} s^{-1} for transfer from biphenyl to Tb^{3+}. The method of converting these rate constants to second-order constants pertaining to the micellar microenvironment is discussed; it is estimated that the transfer process at the micelles is characterized by rate constants about one order of magnitude smaller than the formal ones. The transfer process is thus extremely slow.

Introduction

The early work[1] on energy transfer from excited aromatic ketones and aldehydes, either chelated to rare-earth (RE) ions or as collision partners, clearly showed that the transfer occurred from the triplet state of the sensitizer. It was also shown that the triplet energy of the sensitizer had to be greater than or close to the energy of the acceptor level of the rare-earth ion. In these respects the energy transfer process appeared to be similar to what had been observed in other triplet-triplet transfer reactions.[2,3] Later,[4,5] when collisional sensitized transfer was studied on a time-resolved basis, it was found that the second-order rate constants for the energy transfer to the RE ion were in the region of 10^6-10^8 M^{-1} s^{-1}, far below the normal exothermic triplet-triplet transfer rate of 2-5×10^9 M^{-1} s^{-1}.

Subsequent work[6-8] on rare earth/aromatic aldehyde (and ketone) systems postulated that a complex between the excited sensitizer and the RE ion was formed prior to energy transfer, and that the length of time this complex existed governed the rate of the transfer reaction.[8]

Energy transfer from aromatic hydrocarbon triplets to RE ions had not been observed in fluid solution until recently (Fendler et al.).[9] It was shown that triplet naphthalene solubilized in an anionic micelle (sodium lauryl sulfate) was capable of sensitizing Tb^{3+} "bound" to the micelle surface. It was proposed, with some reservations, that the rate-limiting step of the transfer process is the diffusion of the naphthalene in the micelle to an encounter with surface-bound Tb^{3+}. In solution without the presence of a surfactant no sensitization of Tb^{3+} was observed. This result was attributed to naphthalene triplet-triplet annihilation reactions competing with the energy-transfer process.

† Department of Physical Chemistry, Chalmers University of Technology, FACK, S-40220 Gothenburg, Sweden.
‡ Document No. NDRL-1927 from the Notre Dame Radiation Laboratory.

0002-7863/79/1501-2021$01.00/0